PERGAMON

International Journal of Multiphase Flow 27 (2001) 911–928

International Journal of Multiphase Flow

www.elsevier.com/locate/ijmulflow

A modeling of in-tube condensation heat transfer for a turbulent annular film flow with liquid entrainment

J.T. Kwon [a,*], Y.C. Ahn [b], M.H. Kim [b,1]

[a] *School of Automotive and Mechanical Engineering, Nambu University, 864-1 Wolgye-dong, Kwangsan-gu, Kwangju 506-302, South Korea*

[b] *Department of Mechanical Engineering, Pohang University of Science and Technology, San31 Hyoja-dong, Nam-gu, Pohang 790-784, South Korea*

Received 2 April 1998; received in revised form 16 August 2000

Abstract

An analytical model is developed for condensation heat transfer coefficients for a turbulent annular film flow in tubes. This calculation model not only incorporates a new turbulent eddy viscosity profile modified from the Blangetti and Schlunder model but also liquid entrainment effect. In order to assess the prediction capability of the calculation model, an experiment was performed for measurement of condensation heat transfer coefficients of R22 in horizontal smooth tubes. The calculated condensation heat transfer coefficients of R22 were compared with present experimental data and some existing correlations. From the present analysis and experiment it is found that incorporating the effect of liquid entrainment into the calculation model gives better prediction capability for in-tube condensation heat transfer coefficients. Also, the proposed turbulent eddy viscosity model gives better prediction capability for the condensation heat transfer coefficients than that of the Blangetti and Schlunder model.

Keywords: Analytical model; Condensation; Annular flow; Liquid entrainment; Turbulent eddy viscosity; Turbulent Prandtl number

1. Introduction

Much analytical and experimental research for film condensation has been performed since Nusselt's pioneering work on laminar film condensation (Collier, 1972). For turbulent film

* Corresponding author. Tel.: +82-62-970-0112; fax: +82-62-972-6200.

E-mail addresses: jtkwon@mail.nambu.ac.kr (J.T. Kwon), mhkim@postech.ac.kr (M.H. Kim).

[1] Tel.: +82-54-279-2165; fax: +82-54-279-3199.

0301-9322/01/$ - see front matter
PII: S0301-9322(00)00052-5

condensation, some researchers developed analytical frameworks for solving film hydrodynamics and heat transfer (Colburn, 1933–1934; Seban, 1954; Rohsenow et al., 1956).

Rohsenow et al. (1956) investigated turbulent film condensation by assuming the universal velocity profile in the condensate film and constant turbulent Prandtl number: $Pr_t = 1$. A linear distribution of shear stress between the wall and film surface was used. The local heat transfer coefficient was derived from the energy equation. Also, the effect of vapor shear stress on heat transfer was investigated.

Another approach for the calculation of heat transfer during turbulent film condensation was worked out by Dukler (1960). He also assumed $Pr_t = 1$ but, unlike the method of Rohsenow, turbulent diffusivity for the momentum of the Deissler model in the near-wall region and Karman's model in the region far from the wall were used, respectively. By solving conservation equations for the condensate film, condensation heat transfer coefficients were obtained.

Levich (1962) proposed the eddy damping theory on the free surface. Lamourelle and Sandall (1972) extended the theory through an absorption experiment. Mills and Chung (1973) developed a turbulent eddy viscosity model using the Lamourelle and Sandall's experimental result. Blangetti and Schlunder (1978) suggested a turbulent eddy viscosity model by adopting the van Driest-type model for the wall region and the Levich-type model for the interface region in the liquid film. Chitti and Anand (1995) presented an analytical model based on annular flow for predicting the local heat transfer coefficient for forced convective condensation inside smooth horizontal tubes. They used van Driest-type eddy viscosity model across the condensate film with von Karman's velocity profile. They also used constant turbulent Prandtl number (0.9), and considered no entrainmment case. Kwon and Kim (1998) proposed a modified form of eddy model from Blangetti and Schlunder for the calculation of in-tube condensation heat transfer coefficient of some refrigerants and compared the calculation result with existing experimental data and correlations.

There have been studies for the turbulent Prandtl number model (Jischa and Rieke, 1979; Kays and Crawford, 1980; Weigand et al., 1997). In order to investigate the effect of the turbulent Prandtl number on the heat transfer coefficient of turbulent condensate film, these turbulent Prandtl number models were tested by our calculation model for in-tube condensation heat transfer.

When the vapor velocity is large, the liquid interface becomes wavy and liquid entrainment occurs. By this mechanism, the liquid film thickness becomes thin. Hence, the condensation heat transfer coefficient becomes large (Whalley, 1987). For the calculation of the in-tube condensation heat transfer coefficient for refrigerant flow, the liquid droplet entrainment has not been adopted in previous calculation models. This paper has taken the effect of entrainment into the calculation model for in-tube condensation heat transfer coefficient of refrigerants. This paper also proposes a new turbulent eddy viscosity model within a condensate film, and investigates the effects of turbulent eddy viscosity models and turbulent Prandtl number models on condensation heat transfer.

In order to assess the prediction capability of our calculation model, an experiment was performed to measure condensation heat transfer coefficients of R22 in horizontal smooth tubes. The calculation results for local in-tube condensation heat transfer coefficients of R22 were compared with the present experimental data and existing correlations.

2. Analysis

2.1. Assumptions

The following assumptions are made for the calculation of in-tube condensation heat transfer coefficients for a turbulent annular film flow.

1. Steady flow and heat transfer.
2. Annular film thickness is uniform around the tube circumference. Since the turbulent film has much more dominant effect of inertia than that of gravity in the film, this assumption is possible.
3. Annular film has an equivalent smooth film thickness corresponding to the average wavy film thickness.
4. The convective terms in momentum and energy equations are neglected.

2.2. Momentum conservation

By applying a force balance to an annular element shown in Fig. 1 of the condensate film and pertinent vapor volume between the tube sections at z and Δz, shear stress can be represented by

$$\tau = \frac{R-y}{2}\left(\rho_L g \sin\theta - \frac{dp}{dz}\right) - g\sin\theta(\rho_L - \rho_G)\frac{(R-\delta)^2}{2(R-y)}, \tag{1}$$

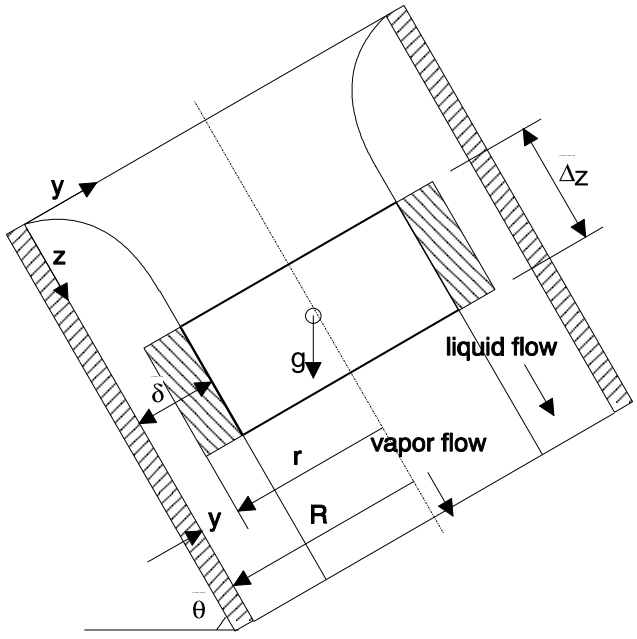

Fig. 1. Physical model for analysis of condensation heat transfer.

where θ denotes the inclined angle from horizontal plane, i.e., $\theta = 0°$ for horizontal flow, $\theta = 90°$ for vertical flow, and δ is the film thickness. Therfore, the interfacial shear stress τ_i can be calculated by substituting δ into y of Eq. (1).

Total shear stress consists of laminar and turbulent parts

$$\tau = \rho_L(v_L + \varepsilon_M)\frac{du}{dy} = \rho_L v_L \varepsilon^+ \frac{du}{dy}, \tag{2}$$

where ρ_L is the density of liquid film, and ε^+ is defined as $\varepsilon^+ = 1 + (\varepsilon_M/v_L)$, also ε_M and v_L are turbulent eddy viscosity and molecular kinematic viscosity, respectively.

By integrating Eq. (2) with the expression of τ (Eq. (1)), the velocity profile can be obtained

$$u = \int_0^\delta \frac{\tau}{\varepsilon^+ \rho_L v_L}\, dy. \tag{3}$$

For the integration, it is necessary to calculate the total pressure gradient and it is represented by

$$\frac{dp}{dz} = \left(\frac{dp}{dz}\right)_f + \left(\frac{dp}{dz}\right)_m + \left(\frac{dp}{dz}\right)_g. \tag{4}$$

The friction term (frictional pressure gradient) can be described as follows

$$\left(\frac{dp}{dz}\right)_f = -\frac{4\tau_w}{d}, \tag{5}$$

where d is tube inner diameter and τ_w is wall shear stress.

Also, the momentum change term (pressure gradient due to the momentum change between phases) follows (Hewitt and Hall-Taylor, 1970; Carey, 1992) when considering liquid entrainment

$$\left(\frac{dp}{dz}\right)_m = -\dot{m}^2 \frac{d}{dz}\left[\frac{x^2}{\varepsilon\rho_G} + \frac{(1-E)^2(1-x)^2 x}{\rho_L(1-\varepsilon)x - \rho_G \varepsilon E(1-x)} + \frac{E(1-x)x}{\varepsilon\rho_G}\right], \tag{6a}$$

where $\dot{m}$ is the total mass flux, x is mass quality, ε is void fraction, and E is liquid entrainment fraction defined as the ratio of the liquid droplet flow rate to the total liquid flow rate. When the liquid entrainment is neglected, Eq. (6a) becomes

$$\left(\frac{dp}{dz}\right)_m = -\dot{m}^2 \frac{d}{dz}\left[\frac{x^2}{\rho_G \varepsilon} + \frac{(1-x)^2}{\rho_L(1-\varepsilon)}\right]. \tag{6b}$$

Since the following assumptions are generally possible for annular two-phase flows inside tubes

$$\rho_G \ll \rho_L, \quad \delta \ll d, \quad \frac{d\varepsilon}{dz} \ll \frac{dx}{dz}.$$

Eq. (6b) becomes

$$\left(\frac{dp}{dz}\right)_m \cong -\frac{2xd^2\dot{m}^2}{\rho_G(d-2\delta)^2}\frac{dx}{dz}, \tag{7}$$

where dx/dz can be obtained from the energy balance

$$\frac{dx}{dz} = \frac{4\dot{q}}{d\dot{m}h_{LG}} = \frac{4h(T_{sat} - T_w)}{d\dot{m}^2 h_{LG}}, \tag{8}$$

where $\dot{q}$ is heat flux, h_{LG} is specific latent heat, and h is local heat transfer coefficient. Also, T_{sat} and T_w are temperatures of saturated fluid and tube wall.

Furthermore, the wall shear stress for turbulent film flow is obtained from

$$\tau_w = f_L \frac{\dot{m}^2(1-x)^2}{2\rho_L}\phi_L^2, \tag{9}$$

where

$$f_L = 0.079 Re_f^{-0.25}. \tag{10}$$

Also, the two-phase friction multiplier ϕ_L^2, and Martinelli parameter X_{tt} are defined as

$$\phi_L^2 = 1 + \frac{20}{X_{tt}} + \frac{1}{X_{tt}^2}, \tag{11}$$

$$X_{tt} = \left(\frac{\rho_G}{\rho_L}\right)^{0.5}\left(\frac{\eta_L}{\eta_G}\right)^{0.1}\left(\frac{1-x}{x}\right)^{0.9}, \tag{12}$$

where η_L and η_G are the dynamic viscosities of liquid and vapor, respectively.

The gravity term (gravitational pressure gradient) is represented by

$$\left(\frac{dp}{dz}\right)_G = [(1-\varepsilon)\rho_L + \varepsilon\rho_G]g\sin\theta. \tag{13}$$

Once the total pressure gradient and the shear stress terms are determined, velocity distribution can be obtained from Eq. (3) with appropriate turbulent eddy viscosity model ε^+. Eqs. (2) and (3) can be represented in dimensionless forms

$$\frac{du^+}{dy^+} = \frac{\tau/\tau_w}{1 + \varepsilon_M/\nu_L}, \tag{14}$$

$$u^+ = \int_0^{y^+} \frac{\tau/\tau_w}{\varepsilon^+}\, dy^+, \tag{15}$$

where the nondimensional variables are defined as dimensionless velocity

$$u^+ = u/u_\tau, \tag{16}$$

dimensionless wall distance

$$y^+ = yu_\tau/\nu_L, \tag{17}$$

and friction velocity

$$u_\tau = \sqrt{\tau_w/\rho_L}. \tag{18}$$

2.3. Mass conservation

Condensate mass flow rate per unit of circumference Γ is calculated by

$$\Gamma \equiv \int_0^\delta \rho u \, \mathrm{d}y = \frac{\dot{m}(1-x)(1-E)d}{4}. \tag{19}$$

Also, film Reynolds number is given by

$$Re_\mathrm{f} = \frac{\dot{m}(1-x)(1-E)d}{\eta_\mathrm{L}} = \frac{4\Gamma}{\eta_\mathrm{L}} = \frac{4}{\eta_\mathrm{L}} \int_0^\delta \rho u \, \mathrm{d}y. \tag{20}$$

2.4. Energy conservation

Under the assumptions of this study, energy equation can be simplified as

$$\frac{\partial}{\partial y}\left[(\kappa_\mathrm{L} + \varepsilon_\mathrm{H})\frac{\partial T}{\partial y}\right] = 0, \tag{21}$$

where κ_L and ε_H are the thermal diffusivity of liquid and turbulent eddy diffusivity for heat, respectively.

Or, it can be represented by

$$\dot{q} = -\rho_\mathrm{L} c_{\mathrm{p,L}} \kappa_\mathrm{L}\left(1 + \frac{\varepsilon_\mathrm{H}}{\kappa_\mathrm{L}}\right)\frac{\mathrm{d}T}{\mathrm{d}y}. \tag{22}$$

Eq. (22) can be written in nondimensional form as follows

$$\frac{\dot{q}}{\dot{q}_\mathrm{w}} = \left(\frac{1}{Pr} + \frac{1}{Pr_\mathrm{t}}\frac{\varepsilon_\mathrm{M}}{\nu_\mathrm{L}}\right)\frac{\mathrm{d}T^+}{\mathrm{d}y^+}, \tag{23}$$

where molecular Prandtl number and turbulent Prandtl number are defined as $Pr = \nu_\mathrm{L}/\kappa_\mathrm{L}$ and $Pr_\mathrm{t} = \varepsilon_\mathrm{M}/\varepsilon_\mathrm{H}$, respectively. Also, the dimensionless temperature and the wall heat flux are represented by

$$T^+ \equiv \rho_\mathrm{L} c_{\mathrm{p,L}} u_\tau / \dot{q}, \dot{q}_\mathrm{w} \equiv h(T_\mathrm{sat} - T_\mathrm{w}). \tag{24}$$

Heat transfer coefficient h is, therefore, expressed as

$$h = \frac{\rho_\mathrm{L} c_{\mathrm{p,L}} u_\tau}{T_\delta^+}, \tag{25}$$

where

$$T_\delta^+ = \int_0^{\delta^+}\left[\frac{\dot{q}/\dot{q}_\mathrm{w}}{(1+Pr) + (1/Pr_\mathrm{t})(\varepsilon_\mathrm{M}/\nu_\mathrm{L})}\right]\mathrm{d}y^+, \tag{26}$$

and

$$\frac{\dot{q}}{\dot{q}_\mathrm{w}} = \frac{A_\mathrm{w}}{A} = \frac{R}{r} = \frac{R}{R-y} = \frac{1}{1-(y^+/R^+)}.$$

2.5. Turbulent eddy viscosity models within liquid film

Blangetti and Schlunder (1978) used a van Driest-type model for the near-wall region and a Levich-type model for the near-interface region as shown in Eqs. (27a) and (27b) for the calculation of in-tube condensation heat transfer coefficients for a vertical film flow.

$$\varepsilon^+ = 0.5 + 0.5\sqrt{1 + 0.64y^{+2}[1 - \exp(-y^+/26)]^2} \quad \text{for } 0 < y^+ < y^*, \tag{27a}$$

and

$$\varepsilon^+ = 1 + 0.0161\, Re_f^{1.345} Ka^{1/3} \left[\frac{\tau_i}{(\rho_L - \rho_G)gl} + \frac{\delta - y}{l}\right](\delta^+ - y^+) \quad \text{for } y^* < y^+ < \delta^+, \tag{27b}$$

where y^* is the matching point where the near-wall and near-interface eddy profiles intersect, and Ka is Kapitza number defined as $Ka = (\rho_L g l^2/\sigma)^3$, where the characteristic length l is defined as $l = (v_L^2/g)^{1/3}$.

The Blangetti and Schlunder model describes the physical situation of turbulent eddy viscosity profile within the film as a two-layer model. They show that their calculation results agree well with their experimental data for steam condensation in vertical tube when the film Reynolds number ranges from 50 to 2000 and the interfacial shear is not too large.

When the film Reynolds number is larger than two thousand, or the nondimensional film thickness reaches the order of 100 or above, this kind of two-layer model is not likely to account for the fully turbulent region in the liquid film since the van Driest model is not applicable to the region of y^+ larger than about 30. In this region, the turbulent eddy viscosity is known to grow moderately and then become nearly uniform.

Therefore, in this study, the van Driest-type model is used only when y^+ is less than 30, and in the region above, as an attempt to form the simplest modeling, the value of eddy viscosity at $y^+ = 30$ is used until it intersects the interface eddy profile. Fig. 2 describes the model proposed in this study.

$$\varepsilon^+ = 0.5 + 0.5\sqrt{1 + 0.64y^{+2}[1 - \exp(-y^+/26)]^2} \quad \text{for } 0 < y^+ < 30, \tag{28a}$$

$$\varepsilon^+ = \varepsilon^+\Big|_{y^+=30} \quad \text{for } 30 < y^+ < y^*, \tag{28b}$$

$$\varepsilon^+ = 1 + 0.0161\, Re_f^{1.345} Ka^{1/3} \left[\frac{\tau_i}{(\rho_L - \rho_G)gl} + \frac{\delta - y}{l}\right](\delta^+ - y^+) \quad \text{for } y^* < y^+ < \delta^+. \tag{28c}$$

2.6. Turbulent Prandtl number models

Three models are tested for the turbulent Prandtl number effects on condensation heat transfer. First the constant turbulent Prandtl number (0.9) is considered. Second, the Jischa and Rieke (1979) model is used, and finally the extended Kays and Crawford model (Weigand et al., 1997) is applied to the calculation. Jischa and Rieke proposed the turbulent Prandtl number as a function of the Reynolds number and the molecular Prandtl number as follows:

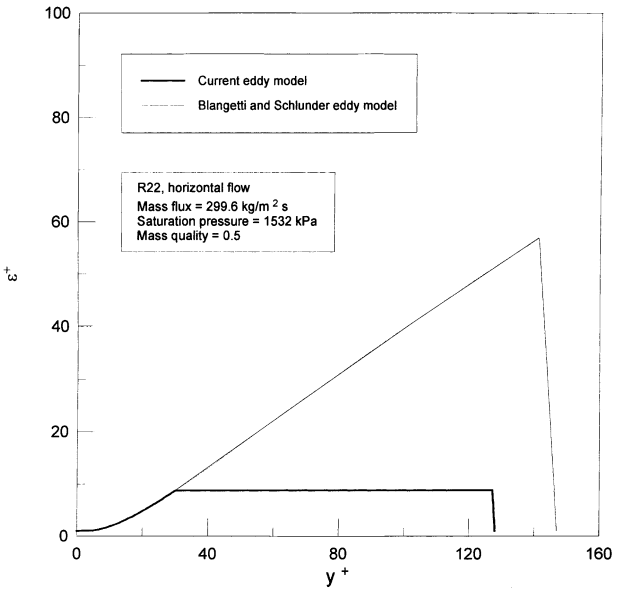

Fig. 2. Typical turbulent eddy profiles in this study.

$$Pr_t = 0.9 + \frac{182.4}{PrRe^{0.888}}. \tag{29}$$

Kays and Crawford suggested a conduction model for the turbulent Prandtl number as a function of the relative wall distance y^+ (Kays and Crawford, 1980).

$$Pr_t = \frac{1}{\frac{1}{2Pr_{t\infty}} + CPe_t\sqrt{\frac{1}{Pr_{t\infty}}} - (CPe_t)^2\left[1 - \exp\left(-\frac{1}{CPe_t\sqrt{Pr_{t\infty}}}\right)\right]}, \tag{30}$$

where $Pe_t = Pr(\varepsilon_M/\nu_L)$, $Pr_{t\infty}$ is the value of Pr_t far from the wall (an experimental constant), and C is an experimental constant.

Also, Weigand et al. (1997) suggested an extended Kays and Crawford model by combining the above two models. They used $Pr_{t\infty}$ like the Jischa and Rieke model as follows:

$$Pr_{t\infty} = 0.85 + \frac{D}{PrRe^{0.888}}, \tag{31}$$

where $D = 100$ was used in their calculation. The extended Kays and Crawford model describes the turbulent Prandtl number dependency on y^+ as well as the Reynolds number and the molecular Prandtl number. In this paper, the effect of these models on condensation heat transfer is discussed.

2.7. Liquid entrainment fraction

For the annular two-phase flow, depending on the condition of vapor and liquid mass flux, liquid droplet entrainment may be very important to the mass, momentum, and heat transfer. The

entrainment process is closely associated with the presence of waves. Even though it is very difficult to measure rates of entrainment from a film in annular flow, many experiments have been conducted to suggest data and correlations for liquid entrainment fraction or entrainment rate.

Paleev and Filipovich (1966) carried out an experiment for measuring the quantities of separated liquid deposited on the wall of a rectangular channel from the turbulent air–water dispersed-annular flow. They used the dimensionless gas flow to express the correlation for the rate of entrainment. Wallis (1969) proposed a correlation for the rate of entrainment. He neglected the effect of viscosity force of liquid phase but introduced the critical gas velocity at which droplet entrainment from the film takes place. Ishii and Mishima (1989) developed a correlation for the amount of entrained liquid in annular flow for the equilibrium and entrance regions. Hewitt and Govan (1990) presented models for deposition and entrainment in annular flow.

The correlation of Ishii and Mishima was adopted in this study in order to incorporate the entrainment effect into the calculation model for condensation heat transfer coefficient since this model is known to be more successful in describing the entrainment for different tube diameters and different fluids (Whalley, 1987), and simple to be implemented in a calculation algorithm. The correlation for equilibrium entrainment fraction is as follows:

$$E = \tan h\left(7.25 \times 10^{-7} We^{1.25} Re_{\mathrm{f}}^{0.25}\right), \tag{32}$$

where the effective Weber number for entrainment is defined by Eq. (33)

$$We = \frac{\rho_{\mathrm{G}} j_{\mathrm{G}}^2 d}{\sigma}\left(\frac{\rho_{\mathrm{L}} - \rho_{\mathrm{G}}}{\rho_{\mathrm{G}}}\right)^{1/3}. \tag{33}$$

The superficial velocity for vapor phase j_{G} is defined by Eq. (34)

$$j_{\mathrm{G}} = \frac{\dot{m}x}{\rho_{\mathrm{G}}}. \tag{34}$$

2.8. Calculation algorithm

This algorithm gives the velocity distribution within the film, condensate film thickness, local condensation heat transfer coefficient, and local pressure drop values. The algorithm is summarized here briefly.

For a specified mass quality x, and total mass flux $\dot{m}$:

1. Calculate the liquid entrainment fraction E, and guess the value of δ^+.
2. Using turbulent eddy viscosity $\varepsilon^+(y^+)$, determine velocity distribution $u^+(y^+)$ by integrating Eq. (14).
3. Calculate the wall shear stress τ_{w} using Eq. (9) for the guessed δ^+.
4. Using Eq. (8), calculate $\mathrm{d}x/\mathrm{d}z$, and determine $\mathrm{d}p/\mathrm{d}z$, τ_{w}, and u_τ, respectively.
5. Check if the mass conservation Eq. (19) is satisfied.
6. If not, return to step (1) again and repeat the same procedure until correct δ^+ is found.
7. Once the value of δ^+ is found, calculate T_δ^+, and h, respectively, using Eqs. (26) and (25).

A Gaussian quadrature method was used for the numerical integration in this calculation.

3. Experiment

In order to assess the calculation modeling, an experiment was performed for the condensation heat transfer of R22 in horizontal smooth tubes. Experimental apparatus and the data reduction method are described briefly here. A detailed experimental method and procedure are shown in Kwon et al. (2000).

3.1. Experimental apparatus

Fig. 3 shows a schematic of the present experimental apparatus. Refrigerant R22 was circulated by a magnetic gear pump. After being heated by the main heater and auxiliary heater, the refrigerant vapor flowed into the test condenser. Cooling water from the constant temperature water bath flowed counter-currently through the annular space of the test section. Seven test sections were connected in series.

A test section consisted of a copper tube and its outer annulus device that is made of acrylic resin. A detail of the test section is shown in Fig. 4. Inside the test tube, the refrigerant flow was condensed by the outer cooling water flow through the annulus.

For each test section, the inlet and outlet temperatures of the refrigerant and cooling water were measured by T-type thermocouples. The thermocouples were calibrated by a precision RTD thermometer and sensor. The accuracy of the calibrated thermocouples was 0.03 K. Also, the volumetric flow meters used for measuring refrigerant and cooling water flow rates were calibrated by measuring the mass collected during a specific period of time. Therefore, the accuracy can be 1% of the full scale of the rotameters.

3.2. Data reduction method

Fig. 5 represents the schematic of a test condenser unit. From an energy balance, Eq. (35) is obtained

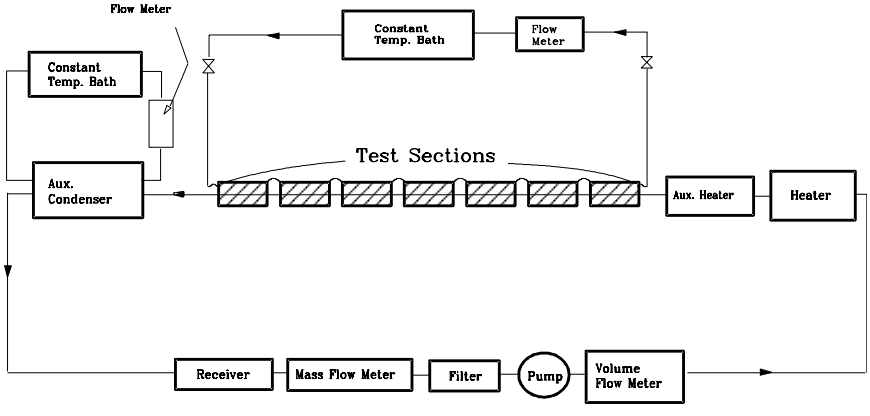

Fig. 3. Schematic of the present experimental apparatus.

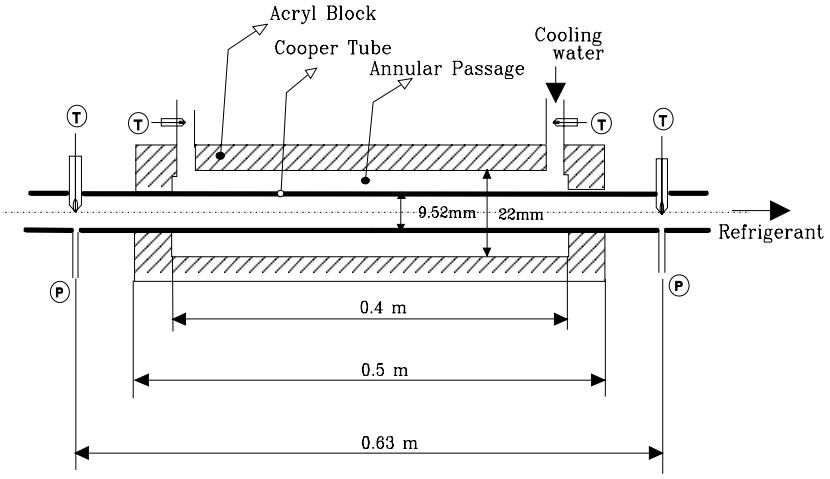

Fig. 4. Detail of a test section.

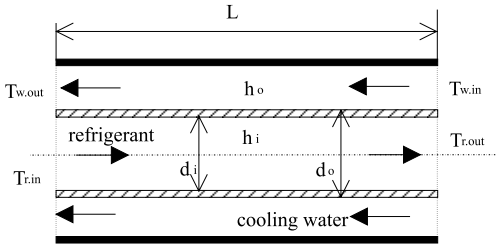

Fig. 5. Schematic of a test section.

$$\frac{1}{U_o A_o} = \frac{1}{h_i A_i} + \frac{1}{h_o A_o} + \frac{\ln(d_o/d_i)}{2\pi k_w L}, \tag{35}$$

where U_o is the overall heat transfer coefficient, h_i is the condensation heat transfer coefficient in tubes, and h_o is the single-phase heat transfer coefficient in the annulus. Also, k_w is the thermal conductivity of copper tube, d_i and d_o are the inner and outer tube diameters, and L is the heat transfer length. From Eq. (35) the in-tube condensation coefficient can be represented by Eq. (36)

$$h_i = \frac{1}{\left[\frac{1}{U_o A_o} - \frac{1}{h_o A_o} - \frac{\ln(d_o/d_i)}{2\pi k_w L}\right] A_i}. \tag{36}$$

The overall heat transfer coefficient is given by Eq. (37)

$$U_o = \frac{Q}{A_o \Delta T_{LM}}, \tag{37}$$

where the heat flow rate Q and the logarithmic mean temperature difference ΔT_{LM} are as follows:

$$Q = \dot{m}_w A_w c_{p,w}(T_{w,out} - T_{w,in}), \tag{38}$$

Table 1
A typical uncertainty for present experimental data

Tube	Mass flux (kg/m^2 s)	δ_{h_o} (%)	δ_{U_o} (%)	δ_{h_i} (%)
Smooth	299.6	10	8	12.8
Smooth	402.5	10	6	11.7

$$\Delta T_{LM} = \frac{(T_{r,out} - T_{w,in}) - (T_{r,in} - T_{w,out})}{\ln[(T_{r,out} - T_{w,in})/(T_{r,in} - T_{w,out})]}, \tag{39}$$

where A_w is the cross-sectional area for water flow.

The annulus side single phase heat transfer coefficients are estimated from the correlation developed by Kwon et al. (1997) by using the modified Wilson plot technique. The single-phase heat transfer correlation for the present annulus passage is as follows:

$$Nu_{ann} = 0.132\,Re^{0.68}\,Pr^{0.4} \quad (\pm 10\%\ \text{accuracy}) \quad \text{for } 2000 < Re < 10,000. \tag{40}$$

3.3. Uncertainty analysis

Present data reduction equation for the in-tube condensation coefficient is found from Eq. (36). Therefore, its functional form is as follows:

$$h_i = h_i(U_o, h_o). \tag{41}$$

The uncertainty analysis expression (Coleman and Steele, 1989) is represented by the following equation:

$$\left(\frac{\delta_{h_i}}{h_i}\right)^2 = \left(\frac{1}{h_i}\frac{\partial h_i}{\partial U_o}\delta_{U_o}\right)^2 + \left(\frac{1}{h_i}\frac{\partial h_i}{\partial h_o}\delta_{h_o}\right)^2, \tag{42}$$

where δ_{U_o}, δ_{h_o}, and δ_{h_i} are the uncertainties of the heat transfer coefficients for overall, outer annulus, and inner tube sides, respectively.

For the present case, the terms in Eq. (42) are expressed by

$$\frac{\partial h_i}{\partial U_o} = \frac{A_o}{A_i}\left(\frac{h_o}{U_o - h_o}\right)^2 \text{ and } \frac{\partial h_i}{\partial h_o} = -\frac{A_o}{A_i}\left(\frac{U_o}{U_o - h_o}\right)^2. \tag{43}$$

From the above analysis, the uncertainty of in-tube condensation heat transfer coefficient is about 10–13% for 95% confidence interval. A typical uncertainty analysis is shown in Table 1.

4. Results and discussion

4.1. Velocity distribution within condensate film

Fig. 6 shows the velocity distribution across the condensate film of R22 at a mass quality 0.5, mass flux 299.6 kg/m^2 s and condensing pressure 1532 kPa. The current eddy viscosity model gave higher velocities for the region above $y^+ = 30$ than the Balngetti and Schlunder model. As

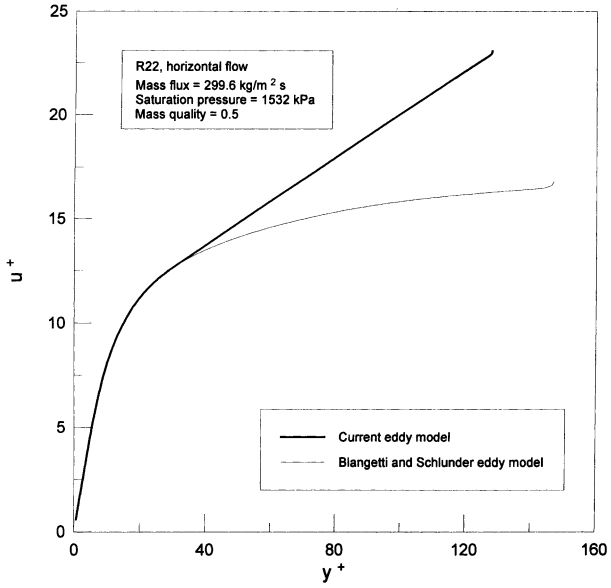

Fig. 6. Velocity profile in condensate film.

shown in Fig. 2, we assumed as a first approximation, the uniform eddy region in the turbulent liquid film. The uniform eddy region resulted in the linear distribution of velocity in the region above $y^+ = 30$. As a result, a higher velocity distribution in this region was obtained and that led to smaller film thickness.

4.2. Film thickness

Fig. 7 represents the nondimensional film thickness of R22 at mass fluxes of 299.6 and 402.5 kg/m^2 s. When mass quality was large, i.e., when condensation began, both the current eddy model and the Blangetti and Schlunder model gave almost the same value of nondimensional film thickness. But the more the condensation proceeds (the smaller the mass quality becomes), the larger the difference will be between the nondimensional film thickness values from the two eddy models. Also, the difference was dominant in the case of high mass flux. The nondimensional film thickness ranged from 30 to 200 in the case of mass flux 299.6 kg/m^2 s, and ranged from 50 to 280 in the case of mass flux 402.5 kg/m^2 s. For these values, the fully turbulent liquid layer may become important for the analysis of film condensation, and the eddy profile of the region seems to have considerable effects on the calculation procedure of film thickness.

4.3. Effects of turbulent Prandtl number

Fig. 8 shows the local condensation heat transfer coefficients when using three different turbulent Prandtl number models at the condition of mass flux 299.6 kg/m^2 s and condensing pressure 1532 kPa. Among them, the extended Kays and Crawford model yielded lower values of heat transfer coefficient than the others. It is due to the turbulent Prandtl number distribution

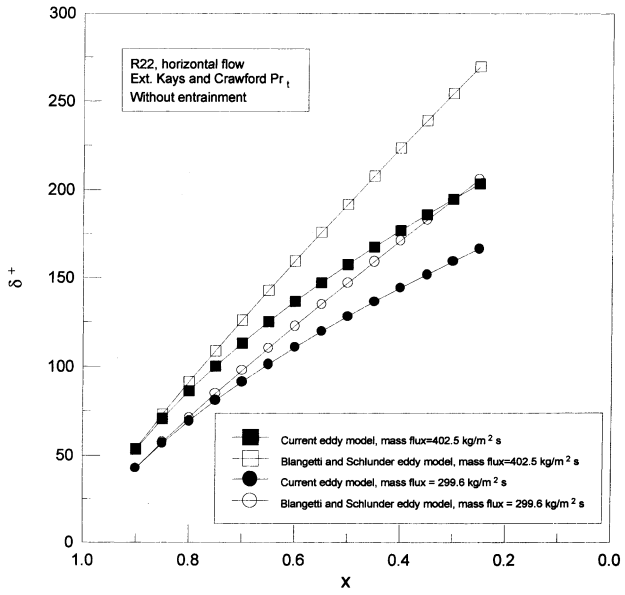

Fig. 7. Nondimensional film thickness variation along mass quality.

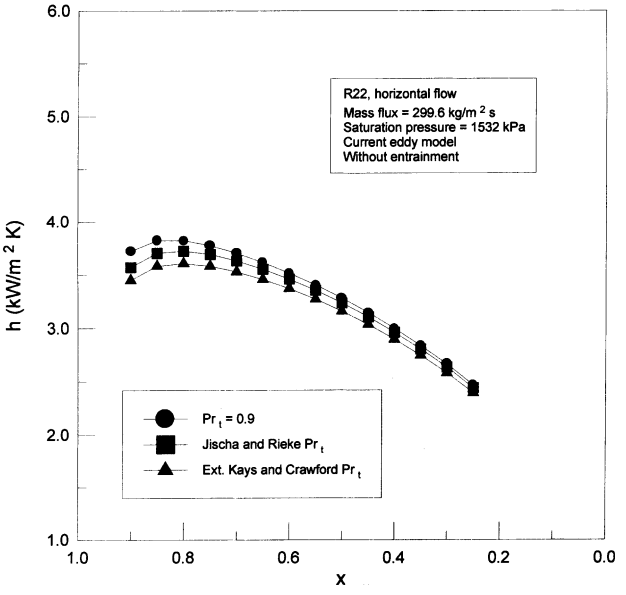

Fig. 8. Effects of turbulent Prandtl number on condensation heat transfer.

along the normal direction of the tube wall. At the region very close to the wall, turbulent eddy conductivity became lower compared with the turbulent eddy viscosity, which means greater thermal resistance for a near-wall layer. This could be described by Kays and Crawford-type

model. The heat transfer coefficients predicted by this model are smaller than those from other models. At the present calculation condition, the predicted values of heat transfer coefficient could be different from each other by 7–8%, especially for high mass quality region.

4.4. Effects of liquid entrainment

Fig. 9 describes the effect of liquid entrainment on condensation heat transfer. Incorporating the liquid entrainment effect into the calculation model gave prominent enhancement of heat transfer, especially for high mass flux and high mass quality region. At the condition of mass flux 299.6 and 402.5 kg/m^2 s, the condensation heat transfer coefficients increased by up to 10% and 20%, respectively.

4.5. Comparison of condensation heat transfer coefficients

In order to verify the prediction capability of our models, the calculated values of condensation heat transfer coefficient in horizontal tubes were compared with the present experimental data and the three existing correlations (Traviss et al., 1973; Cavallini and Zecchin, 1974; Shah, 1979) which are frequently referred to in open literature. The calculation and experimental results of local condensation heat transfer coefficients of R22 in horizontal tubes are shown in Figs. 10 and 11. It is noted that the current eddy model gives a much better prediction capability for condensation heat transfer compared with the Blangetti and Schlunder eddy model.

Fig. 10 shows the comparison of condensation heat transfer coefficients of R22 in horizontal tube at the condition of mass flux 299.6 kg/m^2 s and condensing pressure 1532 kPa. The current

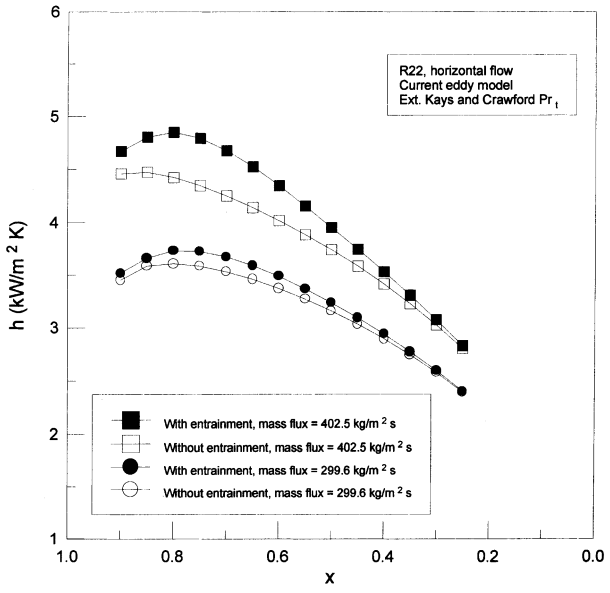

Fig. 9. Effects of liquid entrainment on condensation heat transfer.

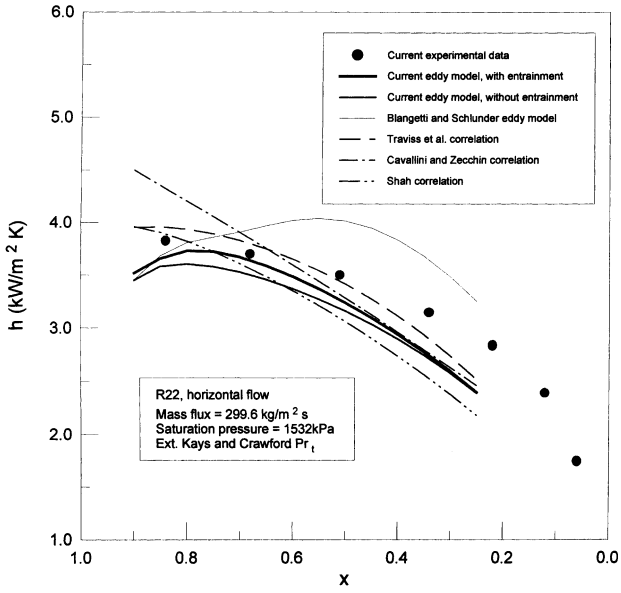

Fig. 10. Comparison of condensation heat transfer coefficients of R22 in horizontal tubes: Mass flux = 299.6 kg/m^2 s, saturation pressure = 1532 kPa.

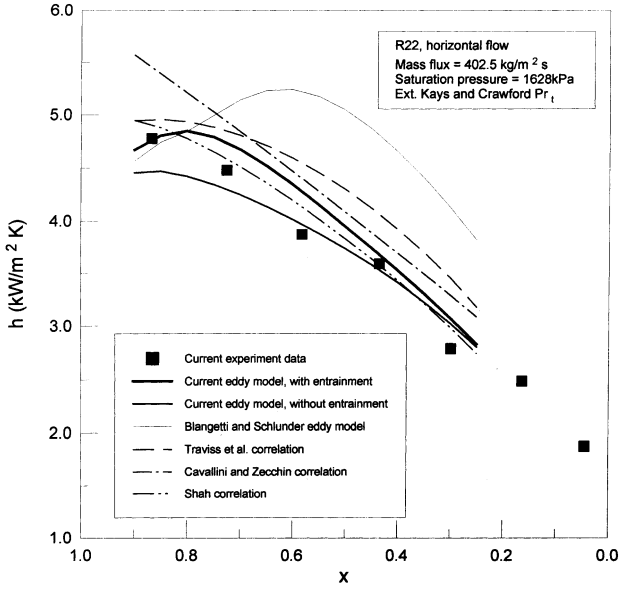

Fig. 11. Comparison of condensation heat transfer coefficients of R22 in horizontal tubes: Mass flux = 402.5 kg/m^2 s, saturation pressure = 1628 kPa.

analytical model slightly underestimated the present experimental data and the values from the existing correlations. Incorporating the liquid entrainment effect gave better prediction capability in this case.

Fig. 11 shows the comparison of condensation heat transfer coefficients of R22 in a horizontal tube at the condition of mass flux 402.5 kg/m^2 s and condensing pressure 1628 kPa. The current analytical model agreed well with the present experimental data as well as the values from the existing correlations.

By comparing the present model with our own experimental data and previous empirical correlations as shown in the Figs. 10 and 11, the incorporation of liquid entrainment effect to calculation model for in-tube condensation heat transfer is highly recommended.

5. Conclusions

For the calculation of the in-tube condensation heat transfer coefficient for turbulent annular film flow, the liquid droplet entrainment has been adopted in order to investigate the effect of entrainment on the condensation heat transfer. A new turblent eddy viscosity model within a condensate film is proposed for the calculation model, and the effects of turbulent Prandtl number models on condensation heat transfer were also discussed.

In order to assess the prediction capability of our calculation model an experiment was performed for the measurement of condensation heat transfer coefficients of R22 in horizontal smooth tubes. And the calculation results for local in-tube condensation heat transfer coefficients of R22 were compared with present experimental data and existing correlations.

From the current analysis and experiment, the following conclusions are drawn:

1. The proposed current eddy viscosity model gives better prediction for condensation heat transfer coefficients compared with the Blangetti and Schlunder model.
2. Incorporating the effect of liquid entrainment into the calculation model for condensation heat transfer makes the prediction capability much better for the condensation heat transfer inside tubes.
3. The prediction capability of the calculation model proposed in this study is confirmed by our present experimental data as well as some correlations frequently referred to for in-tube condensation heat transfer coefficients.

Acknowledgements

This work was carried out with the support of the National Laboratory of Two-Phase Flow and Phase Change Heat Transfer at POSTECH, Korea. The authors are grateful for the support.

References

Blangetti, F., Schlunder, E.U., 1978. Local heat transfer coefficients on condensation in a vertical tubes. In: Proceedings of the Sixth International Heat Transfer Conference, vol. 2, pp. 437–442.

Carey, V.P., 1992. Liquid–Vapor Phase-Change Phenomena. Hemisphere, Washington, DC.

Cavallini, A., Zecchin, R., 1974. A dimensionless correlation for heat transfer in forced convection condensation. In: Proceedings of the Fifth International Heat Transfer Conference, September 3–7, pp. 309–313.

Chitti, M.S., Anand, N.K., 1995. An analytical model for local heat transfer coefficients for forced convective condensation inside smooth horizontal tubes. Int. J. Heat Mass Transfer 38, 615–627.

Colburn, A.P., 1933–1934. Note on the calculation of condensation where a portion of the condensate layer is in turbulent motion. Trans. Inst. Chem. Eng. 30, 187–193.

Coleman, H.W., Steele, W.G., Jr., 1989. Experimentation and Uncertainty Analysis for Engineers. Wiley, New York.

Collier, J.G., 1972. Convective Boiling and Condensation, McGraw-Hill, New York (Chapter 10).

Dukler, A.E., 1960. Fluid mechanics and heat transfer in vertical falling film systems. Chem. Eng. Prog. Symp. Ser. 56, 1–10.

Hewitt, G.F., Govan, A.H., 1990. Phenomenological modelling of non-equilibrium flows with phase change. Int. J. Heat Mass Transfer 33, 229–242.

Hewitt, G.F., Hall-Taylor, N.S., 1970. Annular Two-Phase Flow. Pergamon Press, Oxford.

Ishii, M., Mishima, K., 1989. Droplet entrainment correlations in annular two-phase flow. Int. J. Heat Mass Transfer 32, 1835–1846.

Jischa, M., Rieke, H.B., 1979. About the prediction of turbulent Prandtl and Schmidt numbers. Int. J. Heat Mass Transfer 22, 1547–1555.

Kays, W.M., Crawford, M.E., 1980. Convective Heat and Mass Transfer, second ed. McGraw-Hill, New York.

Kwon, J.T., Kim, M.H., 1998. A calculation model for condensation heat transfer of an alternative Refrigerant. In: Proceedings of the 11th International Heat Transfer Conference, vol. 6, Kyongju, Korea, August 23–28, pp. 373–378.

Kwon, J.T., Park, S.K., Kim, M.H., 2000. Enhanced effect of a horizontal micro-fin tube for condensation heat transfer with R22 and R410A. J. Enhanced Heat Transfer 7, 97–107.

Kwon, J.T., Bae, S.W., Kim, M.H., 1997. Measurement of heat transfer coefficients by using Wilson plot Technique. In: Proceedings of the Society of Air-Conditioning and Refrigerating Engineers of Korea, pp. 257–261 (in Korean).

Lamourelle, A.P., Sandall, O.C., 1972. Gas absorption into turbulent liquid. Chem. Eng. Sci. 27, 1035–1043.

Levich, V.G., 1962. Physicochemical Hydrodynamics. Prentice-Hall, Englewood Cliffs, NJ.

Mills, A.F., Chung, D.K., 1973. Heat transfer across turbulent falling film. Int. J. Heat Mass Transfer 16, 694–696.

Paleev, I., Filipovich, B.S., 1966. Phenomena of liquid transfer in two-phase annular flow. Int. J. Heat Mass Transfer 9, 1089–1093.

Rohsenow, W.M., Webber, J.H., Ling, A.T., 1956. Effect of vapor velocity on laminar and turbulent film Condensation. Trans. ASME Ser. C. J. Heat Transfer 78, 1637–1643.

Seban, R.A., 1954. Remarks on film condensation with turbulent flow. Trans. ASME 76, 299–303.

Shah, M.M., 1979. A general correlation for heat transfer during film condensation inside pipes. Int. J. Heat Mass Transfer 22, 547–556.

Traviss, D.P., Rohsenow, W.M., Baron, A.B., 1973. Forced convection condensation in tubes: a heat transfer correlation for condenser design. ASHRAE Trans. 79, 157–165.

Wallis, G.W., 1969. One-Dimensional Two-Phase Flow. McGraw-Hill, New York.

Weigand, B., Ferguson, J.R., Crawford, M.E., 1997. An extended Kays and Crawford turbulent Prandtl number model. Int. J. Heat Mass Transfer 40, 4191–4196.

Whalley, P.B., 1987. Boiling, Condensation, and Gas–Liquid Flow. Clarendon Press, Oxford (Chapter 9).